



Article

# Effects of Surfactants on the Morphology and Properties of Electrospun Polyetherimide Fibers

Ahmed Abutaleb <sup>1,†</sup>, Dinesh Lolla <sup>2,†</sup> , Abdulwahab Aljuhani <sup>3,†</sup>, Hyeon U. Shin <sup>4</sup>, Jonathan W. Rajala <sup>5</sup> and George G. Chase <sup>6,\*</sup> 

<sup>1</sup> Department of Chemical Engineering, Jazan University, Jazan 45142, Saudi Arabia; azabutaleb@jazanu.edu.sa

<sup>2</sup> Biosciences and Water Filtration Division, Parker-Hannifin Corporation, Oxnard, CA 93030, USA; dinesh.lolla@parker.com

<sup>3</sup> Department of Chemical Engineering, Royal Commission Yanbu Industrial College, Yanbu 41912, Saudi Arabia; juhaniab@rcyci.edu.sa

<sup>4</sup> Hyundai Motor Company, Seoul 18280, Korea; hushin@hyundai.com

<sup>5</sup> American Air Filters, Louisville, KY 40223, USA; jrajala@aafintl.com

<sup>6</sup> Department of Chemical and Biomolecular Engineering, The University of Akron, Akron, OH 44325, USA

\* Correspondence: gchase@uakron.edu; Tel.: +1-330-972-7943

† These authors contributed equally to this work.

Academic Editor: Stephen C. Bondy

Received: 1 July 2017; Accepted: 21 August 2017; Published: 5 September 2017

**Abstract:** Electrospun fibers often have beads as byproducts. Bead formation can be substantially minimized by the introduction of additives, such as ionic salts or surfactants, to the electrospinning polymeric solution. Polyetherimide (PEI) fibers were fabricated using electrospinning. Four different additives, Lithium Chloride (LiCl), Sodium Chloride (NaCl), Triton X-100 and Hexadecyltrimethylammonium Bromide (HTAB) were utilized to alter the polymer solution electrical conductivity and surface tensions. The effects of solution conductivity and surface tension on the electrospinning and the thermal, mechanical stability of the polymeric fibers were investigated. Morphology, thermal properties, permeability and mechanical strength of the fiber mats were investigated using Scanning Electron Microscopy (SEM), Thermogravimetric Analysis (TGA), Frazier Permeability Test, and Tensile tester respectively. The addition of 1.5wt.% HTAB was found to be the optimum concentration to produce PEI fibers without beads. The addition of HTAB produced fiber mats with higher air permeability, higher thermal stability and higher mechanical strength in comparison to the other additives. Finally, a filtration test was conducted on a simple custom model to compare the performance of beaded and non-beaded PEI fiber mats. The non-beaded PEI fiber mat performed better in terms of both separation efficiency (%E) and differential pressure drop ( $\Delta P$ ) separating water droplets from diesel fuel.

**Keywords:** polyetherimide; electrospinning; nanofibers; surfactant and filtration

## 1. Introduction

According to the National Science Foundation (NSF), materials with at least one dimension equal to or less than 100 nanometers are defined as nanomaterials [1]. Hence, fibers with diameter less than or equal to 100 nm are considered as nanofibers. This definition is usually broadened in the industry to consider all fibers with submicron diameters as nanofibers. Nanofibers are solid-state linear nanomaterials that are flexible and have an aspect ratio greater than 1000:1 [1]. Nanofibers and nanofiber mats have many outstanding properties such as small fiber diameter [2,3], high aspect ratio

(length to diameter ratio) [4,5], large surface area to volume ratio or mass ratio [6,7], high porosity [4,8], flexibility in surface functionalities [9], small pore size [8,10], and superior directional strength [1].

Nanofibers can be produced using many different techniques such as self-assembly [7,11], template synthesis [7,12], phase separation [9,13], drawing [14,15] and electrospinning [16–20]. These manufacturing processes have advantages for specific fiber formation; however, they have some disadvantages from a processing standpoint. Many researchers consider electrospinning as the most efficient technique for the fabrication of nanofibers [16].

Electrospinning is a technique that utilizes electrical forces to draw jets from polymer solution. The setup is very simple, and the process is fast. Continuous fibers can be easily produced and the scale up of this process seems possible [16–20]. The setup applied in this work is shown in Figure 1. The setup consists of three components: (1) a high voltage power supply (2) a syringe pump with two syringes to deliver polymer solution through flexible polymer tubes to two small diameter needles and (3) a rotating collector.

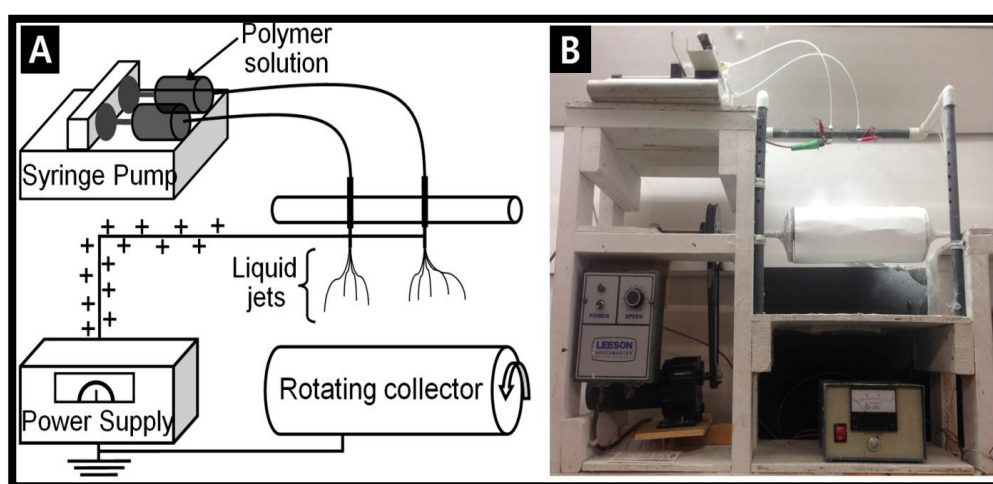


**Figure 1.** A custom fabricated electrospinning setup with two needles. (A) Schematic of electrospinning apparatus and (B) Photograph of the laboratory electrospinning setup.

The syringe pump forces polymer solution to the tip of the charged needles. The electrical charge from the needle induces the charged ions in the polymer solution to move toward the electrode of opposite polarity and cause a polymer jet to launch from the droplet. The jet travels directly toward the opposite charge collector where the nanofibers are collected. The solvent evaporates from the jet and solidified fibers are captured on the collector.

Electrospinning is governed by several processing and operating parameters; slight changes in these factors affect fiber morphology greatly. Generally three different fiber formation phenomena's were observed: unconnected beads, beaded fibers, and non-beaded fibers [21–25]. H. Fong et al. [24] suggested that the beaded fibers are produced due to a capillary breakup of the jet during electrospinning. They also reported that surface tension and viscoelastic properties were the main parameters for bead generation. The net charge density carried by the electrospinning jet, solution viscosity, and surface tension of the polymer solutions are the main factors that influence bead formations [26,27].

Increasing the solution viscosity can form bigger bead, longer average distance between beads, and larger fiber diameters. The size of both beads and fibers become smaller when the net charge density increases. In addition, lowering the surface tension of the polymer solution can reduce the bead concentration or eliminate the beads [24].

Controlling formation of beads, and thus changing the properties of the electrospun fibers, by altering a variety of factors has received attention as a direct consequence of specific requirements

imposed by each application [23,25,28]. These controllable parameters can be divided into three groups: (i) ambient parameters such as humidity, air velocity in the electrospinning chamber, and solution temperature; (ii) process parameters such as hydrostatic pressure in the capillary tube, flow rate, electric potential at the capillary tip, and the gap distance between the needle tip and the collector; and (iii) polymer solution properties such as viscosity, surface tension, conductivity, and elasticity [9,29].

The addition of surfactants and/or salts to the electrospinning polymer solution can enhance the polymer solution properties. In fact, surfactants may have the capability to lower the surface/interfacial tension and salts can increase the electrical conductivity of the polymer solution. L. Yao et al. [30] have reported that the addition of a small amount of Triton X-100, non-ionic surfactant, to the aqueous poly(vinyl alcohol) solution enhanced both the onset voltage and the reproducibility of electrospinning. E. S. Araujo et al. [23] have also proved that the introduction of non-ionic surfactant, Triton X-100, limited bead formation and improved the homogeneity of fiber of the poly(vinyl alcohol) during electrospinning. T. Lin et al. [22] have studied the inclusion of different surfactants on polystyrene electrospinning. They concluded that inclusion of a small amount of cationic surfactant, dodecyltrimethylammonium bromide or tetrabutylammonium chloride, in the polymer solution effectively stopped the formation of beads completely during the electrospinning. They also found that the addition of non-ionic surfactant, Triton X-405, reduced the number of beads, but did not eliminate the beads completely.

K. Nartetamrongsutt et al. [28] tested the influence of salt and solvent concentrations on morphology of electrospun polyvinylpyrrolidone fiber diameters and bead formation. They found that different ionic salts (LiCl, NaCl and MgCl<sub>2</sub>) had different effects on the electrical conductivity behavior of the solutions. D. Fallahi et al. [26] studied the effect of LiCl and non-ionic surfactant on morphology of polystyrene electrospun nanofibers. They concluded that the addition of salt resulted in the fabrication of polystyrene with fine and consistent fibers. Adding 0.1% surfactant reduces the solution surface tension and results in smaller beads and larger fiber diameters. By increasing the amount of surfactant to 0.3%, bigger beads and thinner fibers were produced.

Polyetherimide (PEI), commercial name Ultem, was chosen to investigate the effect of salt and surfactant addition to the polymer solution on the electrospun fiber mat properties. PEI is an amorphous polymer with remarkable thermal, mechanical, and chemical properties. PEI has a glass transition temperature of 217 °C [31]. It is used in many engineering applications such as in separation processes especially separation of helium or hydrogen from other gases and in catalytic reaction processes [16,31,32].

Precipitation, condensation and atmospheric humidity are considered as main sources for water contamination in diesel chambers leading to corrosion, growth of microorganisms and reduced engine life. These emulsified water droplets often possess typical drop sizes ranging from 100 nm to few microns and inseparable using conventional techniques like gravity settling and cyclone separators. Polymeric nanofibers are of great interest in various applications such as catalysis [33,34], wound dressing [29], drug delivery [29], sensor technology [6] and filtration [35]. Nonwoven based superhydrophobic structures are often used as filter media, but not all hydrophobic surfaces interact with emulsified mixture to achieve effective separation efficiency. S. U. Patel et al. [36] studied the water contact angles with hysteresis and effect of basis weight of filter media on separation efficiency using electrospun Poly(vinylidene fluoride-co-hexafluoropropylene) PVDF-HFP. G. Viswanadam et al. [37] studied contact angles of tiny water droplets on PVDF-HFP, polypropylene electrospun fibers on curved tubular springs and used them as tubular coalescers and compared their performance over flat sheet media. X. Yang et al. [38] further assisted superhydrophobic tubular media with external vibrations to aid rate of water drop coalescence and studied the effect of filter orientation to gravity and vibrational frequency. D. Lolla et al. [20] studied effects of polarization on electrical and morphological properties electrospun PVDF fibers and applied in capturing nanoscale solid brine aerosols.

S. C. Moon et al. [39] reported fabrication of aligned PEI fibers over 1 μm in diameter by dissolving 20 wt. % of PEI in 1-methyl-2-pyrrolidinone (NMP), fibers were collected on a rotating cylindrical drum.

S. S. Choi et al. [40] studied interfacial bonding between PEI electrospun fiberwebs with respect to thermal treatment and observed interfiber bonding at 240 °C which substantially enhanced mechanical strengths of the fibers.

In this work, the effects of surface tension and solution conductivity on the morphology and engineering properties of electrospun PEI nanofibers were investigated. Adjustment of surface tension and solution conductivity were achieved by adding different salts and surfactants. Sodium Chloride (NaCl), Lithium Chloride (LiCl) were used to change the conductivity of the solutions. Non-ionic surfactant, Triton X-100, and cationic surfactant, Hexadecyltrimethylammonium Bromide (HTAB), were added to alter the surface tension of the polymer solution. PEI fibers were tested as a barrier filter media to evaluate the effect of beads on separation performance of submicron sized water droplets in diesel fuel. However, there are several other tests needed before we draw an affirmative conclusion to determine the effects of change in water concentration, different fiber size distributions, thickness of the media, volumetric flow-rate and face velocity of diesel fuel. Recirculation test are required to determine the filter life expectancy. A detailed statistical analysis on performance of PEI fibers as filter media for secondary dispersions of water in diesel fuel alone would require to be reported in a whole new research article.

## 2. Experiments

### 2.1. Chemicals

Materials used in this work were Polyetherimide (PEI, commercial name Ultem 1000, MW: 55,000 g/mol, donated by SABIC, 1,1,2-Trichloroethane, (Abbreviated TCE, Sigma Aldrich, St. Louis, MO, USA), Hexadecyltrimethylammonium Bromide (Abbreviated HTAB, Sigma Aldrich, St. Louis, MO, USA), and Triton X-100 (Abbreviated X-100, Sigma Aldrich, St. Louis, MO, USA), Sodium Chloride (Abbreviated NaCl, Fisher Scientific, Hampton, NH, USA) and Lithium Chloride, anhydrous 99% (Abbreviated LiCl, Acro Organics, Geel, Belgium). All chemicals were used as purchased without further purification.

### 2.2. Characterization

#### 2.2.1. Electrical Conductivity and Surface Tension

The electrical conductivities of the solutions were measured using an electrical conductivity meter (Benchtop Orion 3 Star, Thermoscientific, Waltham, MA, USA). The surface tension was measured with a CSC DuNouy Tensiometer. The electrical conductivity and surface tension of each sample were measured three times, and averaged values are reported.

#### 2.2.2. Scanning Electron Microscopy (SEM)

Scanning Electron Microscope (FEI Quanta 200 at 30 kV and HITACHI TM3000 at 15 kV) (FEI, Portland, OR, USA) was used to study the fiber morphology. The average fiber diameter of the nanofibers and the distribution of the fiber diameter were measured directly from the SEM images using FibraQuant software (Version 1.3, nanoScaffold Technologies LLC, Chapel Hill, NC, USA). The distribution of the fiber diameter is displayed in histograms. Each histogram was generated out of more than 100 individual measurements.

#### 2.2.3. Thermogravimetric Analysis (TGA)

The thermal properties and content of whether the additives change the thermal properties of the electrospun fiber web were analyzed with a thermogravimetric analyzer of (TGAQ500) (TA instruments-Waters L.L.C, New Castle, DE, USA). TGA analysis was performed at 30 °C–800 °C with 20 °C/min with controlled liquid nitrogen environment.

#### 2.2.4. Frazier Permeability Test

Frazier Air Permeability Tester (Frazier Precision Instrument Company, Inc., Hagerstown, MD, USA) was used to measure the permeability of each fiber mat. The permeability can be calculated by using Darcy's law. Darcy's law relates the pressure drop to flow through a membrane with the permeability coefficient as given below:

$$Q/A = k(P_0 - P_1) / L \cdot \mu \quad (1)$$

Where Q is the volumetric flow rate in (m<sup>3</sup>/s), A is the area of the membrane in (m), k is the permeability in (m<sup>2</sup>), P<sub>0</sub> and P<sub>1</sub> are the final and initial pressure in (Pa), L is the thickness of the membrane in (m), μ is the kinematic viscosity in NS/m<sup>2</sup>. For thin media, as for the electrospun fiber mats, a precise measure of the thickness of the mat is crucial for obtaining accurate permeability values. Hence, for this work the permeability will be reported based on the ratio of the permeability to the thickness of the medium.

#### 2.2.5. Mechanical Strength Tests

The tensile properties of the electrospun fiber web were generated using a Nano Bionix tensile tester (MTS Systems Corp., Oak Ridge, TN, USA). All fibers were extended at a constant rate of 0.05 S<sup>-1</sup> until the fibers failed. The load required to break the fibers in (mN) was plotted versus the extension that the fibers can be stretched to before they break, in (mm).

#### 2.3. Fabrication of PEI Nanofibers

14 wt. % PEI solutions with different additives percentages, 0.5 wt. %–1.5 wt. %, were prepared by dissolving PEI in TCE in compositions as shown Table 1. Five mL of each solution was loaded into a plastic syringe. Two syringes of each solution were electrospun at the same time as shown in Figure 1. The spinning conditions were 10 mL/min flow rate, 20 kV, and 20 cm gap distance between the needle and grounded electrode (Aluminum foil). The electrospinning was performed at room temperature. LiCl did not dissolve in PEI/TEC polymer solution, thus no experiments were performed to study the effect of LiCl in the PEI nanofiber priorities. Prior to characterizations and usage all the electrospun fiber mats were dried in an oven at 80 °C to ensure evaporation of leftover solvent and additives.

**Table 1.** Surface tension and electrical conductivity of electrospinning solutions. All the readings were obtained at room temperature.

Sample	Surface Tension (dynes/cm)	Electrical Conductivity (μs/cm)
PEI 14 wt. % in TCE without any additive	39 ± 0.29	0.053 ± 0.0026
PEI 14 wt. % in TCE and 1.5 wt. % NaCl	37 ± 0.58	0.07 ± 0.0028
PEI 14 wt. % in TCE and 1.5 wt. % X-100	36.5 ± 0.50	0.4 ± 0.0058
PEI 14 wt. % in TCE and 1.5 wt. % HTAB	36 ± 0.60	4.75 ± 0.15

#### 2.4. Filtration Test

To test the change in performance of PEI without additives and with HTAB, a filtration test was conducted. Electrospun fibers were used in water-diesel separation applications [35,36]. The electrospun fiber mats served as a barrier to the dispersed water drops. In this work, the electrospun fibers had different morphologies and different fiber packing structures. Hence, two types of the electrospun fibers were tested for their efficiency in retaining the dispersed water drops and passing bulk diesel.

The PEI membranes were challenged with a dispersion of water in diesel to study the separation efficiency of the membranes. The dispersion was prepared by mixing 10 mL of deionized water with



6000 mL of diesel. The mixture was circulated by using a centrifugal pump for 10 min prior to filtration testing. The dispersion experimental setup is shown in Figure 2.

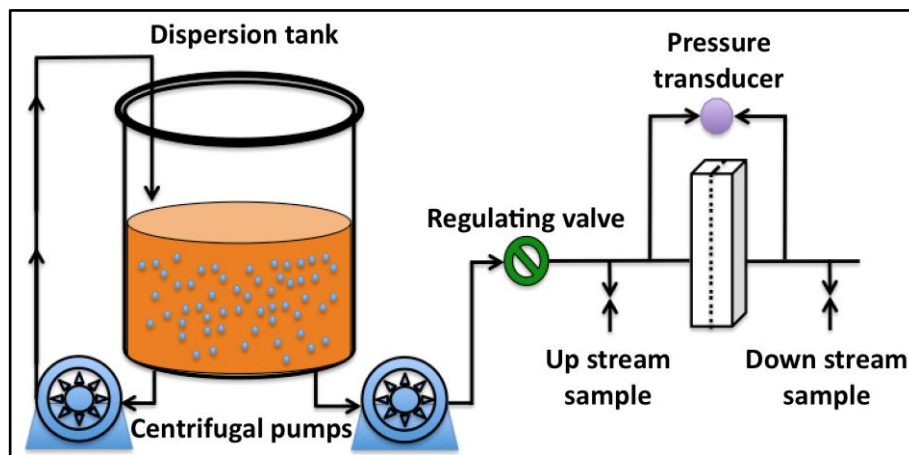


**Figure 2.** Dispersion setup: Two centrifugal pumps were used, the first pump was used for circulating water-diesel mixture in the dispersion tank and the other pump was used to pump the dispersion to the filter medium.

The fiber mats were peeled off the aluminum foil and were placed on stainless steel meshes. The mesh openings were  $400\ \mu\text{m} \times 400\ \mu\text{m}$ . The mesh was used to support the fiber mat and to ensure that the fiber mat does not flex with the direction of the flow.

Maintaining mechanical rigidity of the fiber mat is vital for comparing the performance of the membranes. The mechanical integrity is important for maintaining the fibers orientation and structure. A photograph of the filter holder is shown in Figure 3.

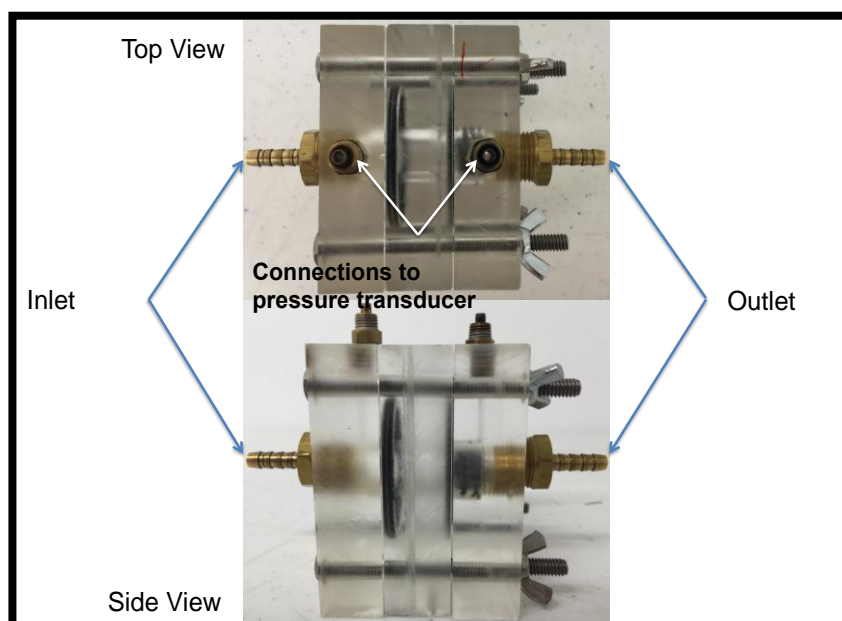


**Figure 3.** Plexiglas filter holder used to conduct liquid-liquid experiments. The holder consists of three pieces, two pieces for the inlet and outlet fittings and the fittings for the pressure transducer. The third piece has O-rings to insure proper sealing. The electrospun membrane is held inside the Plexiglas holder with about 2.2 cm opening diameter available for liquid flow.

Filter media performances are characterized by pressure drop and separation efficiency. The two performances can be characterized by one parameter, the Filtration Index (also known as the Quality Factor). The separation efficiency is given by

$$E = (M_{in} - M_{out})/M_{in} \quad (2)$$

$E$  is the separation efficiency,  $M_{in}$  is the total mass of water drops in the upstream, and  $M_{out}$  is the total mass of water in the downstream. The Filtration Index is defined by

$$FI = -\ln(1 - E)/\Delta P \quad (3)$$

$\Delta P$  is the pressure drop across the filter medium.

### 3. Results and Discussion

Electrospun PEI fiber mats with different additives have different macroscopic structures. The amount of the collected fibers was different for each additive. The most uniform fiber mat was produced when adding HTAB. The average weights per area ( $\text{g}/\text{m}^2$ ) of the fiber mats were 0.254, 0.145  $\text{g}/\text{cm}^2$ , 0.253  $\text{g}/\text{cm}^2$  and 0.297  $\text{g}/\text{cm}^2$  for 14% PEI with no additive, 1.5 wt. % NaCl, 1.5 wt. % X-100, and 1.5 wt. % HTAB respectively. Thus, the amount of the collected fiber increased when adding HTAB. HTAB surfactant not only increased the amount of the collected fibers, but also facilitated electrospinning.

It was obvious from the SEM image in Figure 4 that electrospinning of 14 wt. % PEI in TCE without any additive formed a lot of big beads. These beads were formed due to high surface tension and low electrical conductivity of the polymer solution as shown in Table 1. It was also noticed that electrospinning was difficult and the needle had to be cleaned periodically because the polymer solution dried and solidified at the needle tip.

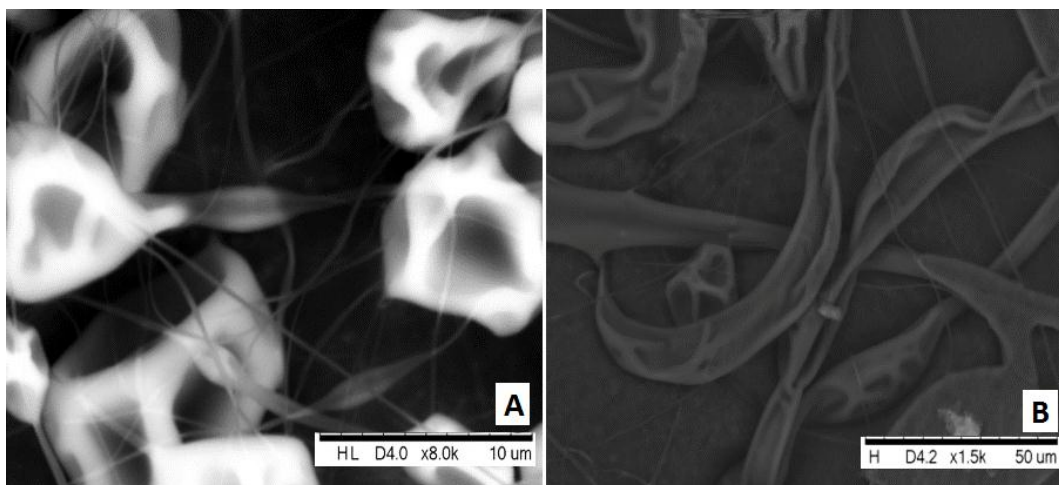


**Figure 4.** SEM images of electrospun fibers of 14 wt. % PEI without any additives at 20 kV, 20 cm and 10  $\mu\text{L}/\text{min}$ .

The addition of different amounts of NaCl, 0.5 wt. %–1.5 wt. %, to the polymer solution increased the PEI polymer solution electrical conductivity and decreased its surface tension slightly as shown in Table 1. Increasing the amount of NaCl to the polymer solution up to 1.5 wt. % could not reduce the formation of beads as shown in Figure 5. The mean average fiber diameters were 0.77  $\mu\text{m}$ , 0.73  $\mu\text{m}$ , and 0.58  $\mu\text{m}$  for 0.5 wt. %, 1 wt. %, and 1.5 wt. % of NaCl in PEI polymer solutions. Thus, the addition of NaCl salt is not a good additive to improve the electrospun PEI morphology as it did not reduce bead formation.

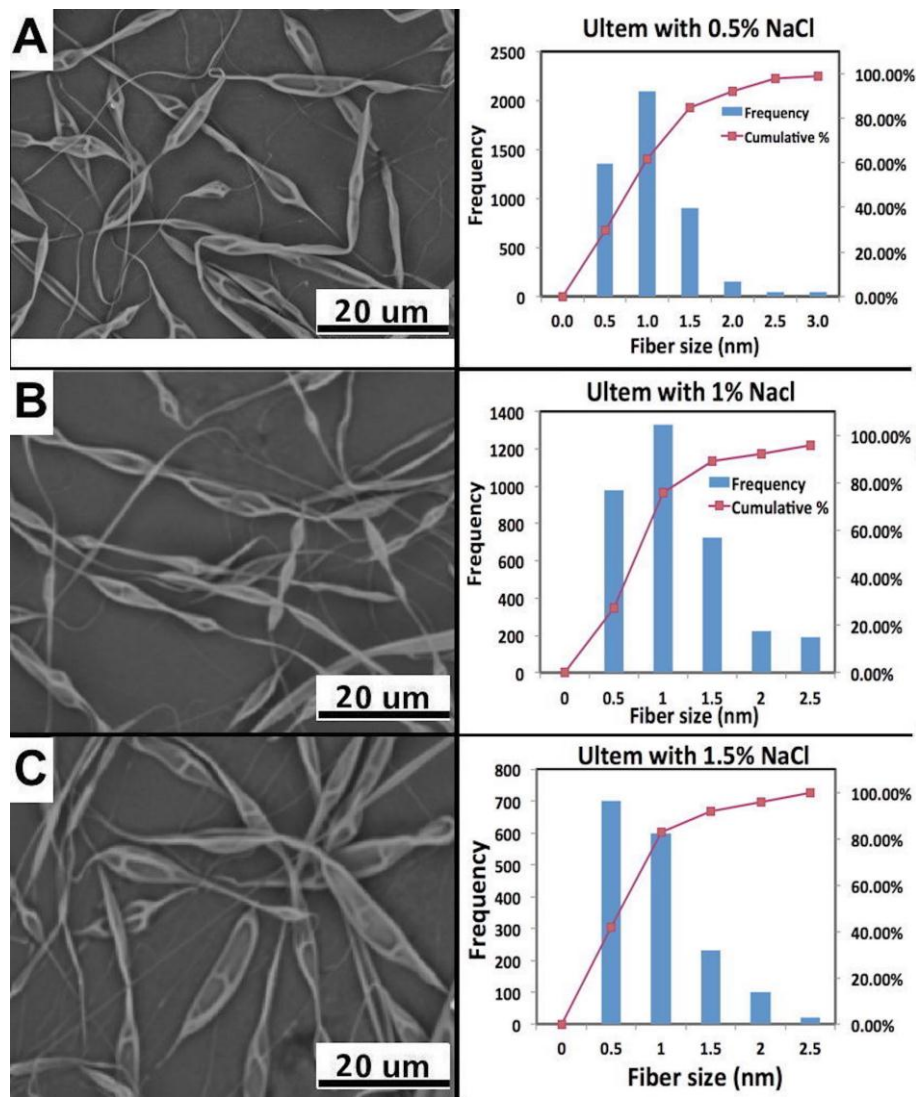


**Figure 5.** SEM images of 14 wt. % PEI and (A) 0.5 wt. % NaCl, (B) 1 wt. % NaCl, (C) 1.5 wt. % NaCl, salt addition electrospun fibers at 20 kV/20 cm and 10  $\mu$ L/min.

When adding different amounts of a nonionic surfactant, Triton X-100, to the polymer solution, the bead formation decreased as the Triton X-100 wt. % increased until it disappeared completely as shown in Figure 6. Surfactant X-100 increased the electrical conductivity of the polymer solution and reduced the surface tension of the polymer solution as shown in Table 1. The fiber average diameters were 1.29  $\mu$ m, 1.24  $\mu$ m, and 1.17  $\mu$ m when adding 0.5 wt. %, 1 wt. %, and 1.5 wt. % of Triton X-100 respectively. The addition of cationic surfactant, HTAB, at 1 wt. % or higher was found to give the best results among salt and surfactants tested here. The beads decreased sharply when adding 0.5 wt. % HTAB, and disappeared completely at 1 wt. % HTAB or higher as shown in Figure 7. The  $f_{\text{mean}}$  average diameters were 0.98  $\mu$ m, 0.78  $\mu$ m, and 0.64  $\mu$ m for addition of 0.5 wt. %, 1 wt. %, and 1.5 wt. % HTAB. It was possible to produce small fibers without beads by introducing small amounts of HTAB surfactant to the polymer solution.



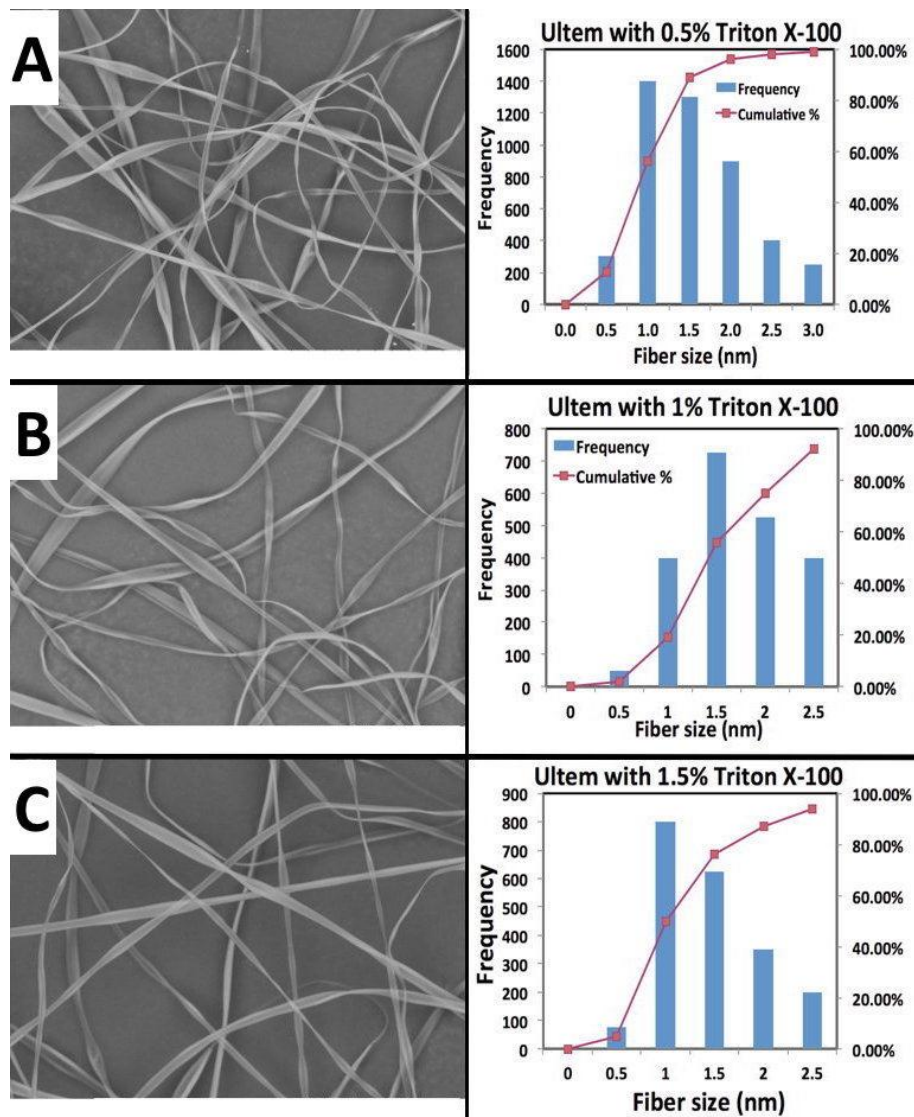


**Figure 6.** SEM images of 14 wt. % PEI and (A) 0.5% Triton X-100, (B), 1% Triton X-100, (C) 1.5% Triton X-100 surfactant addition electrospun fibers at 20 kV/20 cm and 10  $\mu\text{l}/\text{min}$ .

One of the unique characteristics of polyetherimide is its thermal properties. The thermal properties of PEI may be altered due to the additives, so the fiber samples were tested using a TGA. The TGA. Figure 8, indicates that NaCl changed the thermal properties of the PEI fiber mat dramatically. The fiber mat lost its total weight at almost 680  $^{\circ}\text{C}$  when adding 1.5 wt. % NaCl. This result also is in agreement with the low average weight per area ( $\text{g}/\text{m}^2$ ) of the fiber mats, 0.145, when adding NaCl compared to other fiber mats. Thus, the addition of NaCl significantly changed the thermal properties of PEI.

Addition of X-100 also altered the thermal performance of PEI fiber mat but to a lesser extent. The X-100 fiber mat weight was 28% compared to 45% of the non-additive sample at 800  $^{\circ}\text{C}$ . There was almost no change in the thermal performance of PEI when adding HTAB surfactant. This proved that cationic surfactant is the only additive among tested additives that does not affect the thermal properties of PEI fiber mat negatively.

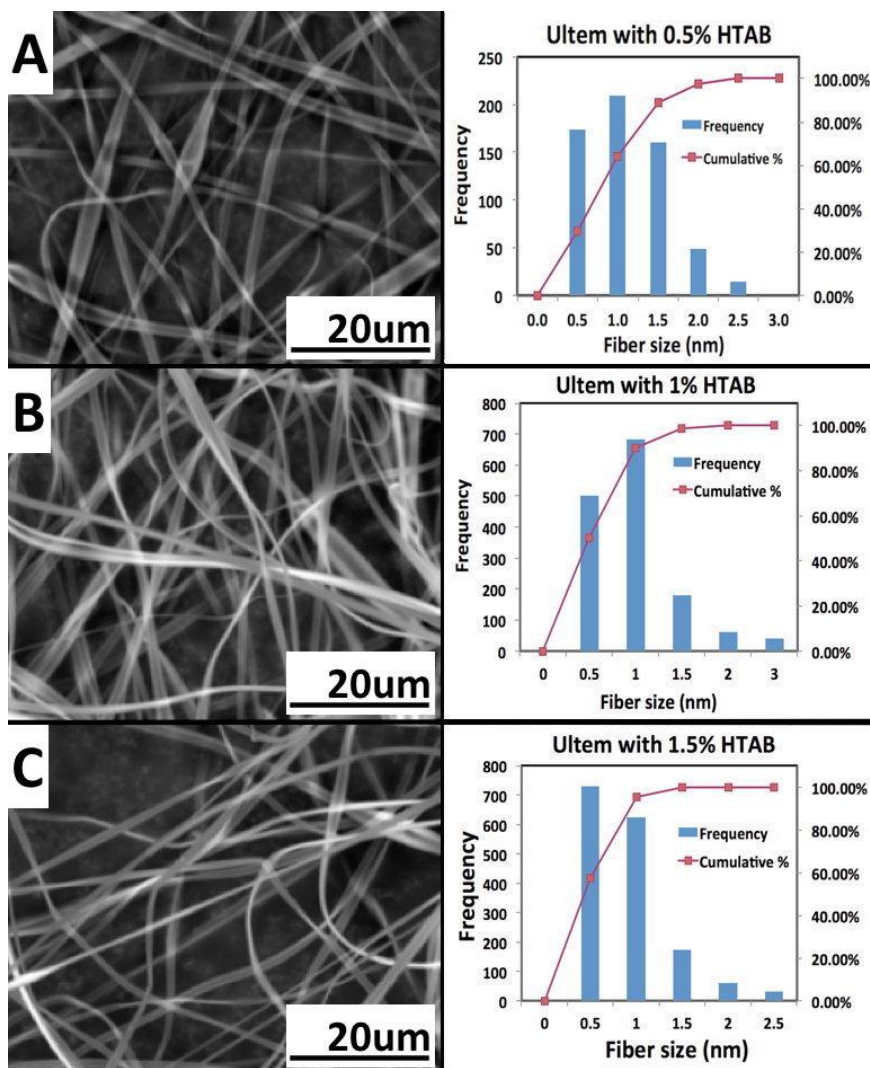


Figure 7. SEM images of 14 wt. % PEI and (A) 0.5 wt. % HTAB, (B) 1 wt. % HTAB, (C) 1.5 wt. % HTAB surfactant addition electrospun fibers at 20 kV/20 cm and 10 μL/min.

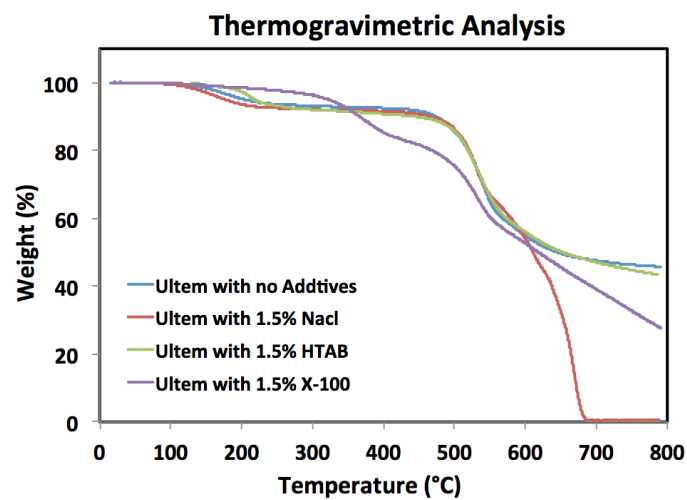


Figure 8. Thermogravimetric analysis of PEI fiber mats with different additives.

Permeability-to-thickness ratios were found to be  $7.274 \times 10^{-6}$  m,  $1.39 \times 10^{-5}$  m,  $1.35 \times 10^{-5}$  m and  $8.236 \times 10^{-5}$  m for PEI fiber mat without additive, with 1.5 wt. % NaCl, with 1.5 wt. % X-100, and with 1.5 wt. % HTAB respectively. It is interpreted that the presence of the beads affected the permeability significantly, by one order of magnitude for the measured samples in this case. The highest permeability-to-thickness ratio was obtained when using HTAB additive because the fibers were small and no beads existed.

Figure 9 shows the amount of load required to break the prepared fiber mats. The loads required to break the fiber mat were around 50 mN, 150 mN, 320 mN and 650 mN for breaking PEI without additive, with 1.5 wt. % NaCl, 1.5 wt. % X-100, and 1.5 wt. % HTAB respectively. It can be concluded that the existence of beads made the fiber mats easier to break. Beaded fibers were fluffier than continuous fibers, hence lamination between fiber web structures was very weak and this made beaded fibers more fragile. HTAB was found to be the best additive to enhance the engineering properties of PEI fiber mats.

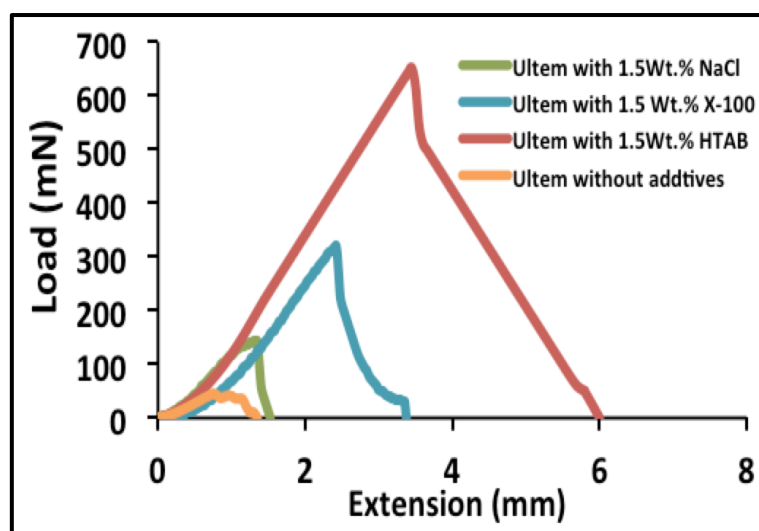


Figure 9. Tensile properties of pure PEI fiber mats and with addition of different surfactants.

The separation efficiency and the FI determine the performance of the filter medium. These two characteristics depend on the structure of the filter medium. The morphology of the electrospun fibers controls the porosity and the permeability of the electrospun mat. The porosity and permeability control the filter performance. Porosity measurements for thin media are very challenging, and were not investigated in this work. The permeability can be affected by the spinning conditions and bead formation as investigated by S.U. Patel et al. [36].

Comparison of Figures 10 and 11 show that the non-beaded fiber media had significantly higher separation efficiency than the beaded fibers. The separation efficiency tests were conducted on three different samples of each medium type in three independent experiments. The efficiencies and filtration indexes of the three tests of each filter were averaged. The average efficiency was  $87\% \pm 10.5\%$  and the average FI was  $11.6 \pm 5$  for the non-beaded fiber mats. The average efficiency was  $62\% \pm 8\%$  and the FI was  $3.7 \pm 1$  for the beaded fiber mats.

These results show that the presence of beads on fiber mats negatively affected the separation efficiency. In addition, the average pressure drop for the non-beaded fiber mat was found to be 0.23 psi versus 0.48 psi for the beaded fiber mat. Hence the FI was negatively affected by the increase in the pressure drop as shown by the beaded fiber mat results. Hence, the filtration performance of the non-beaded fiber mats surpassed the performance of the beaded fiber mats.

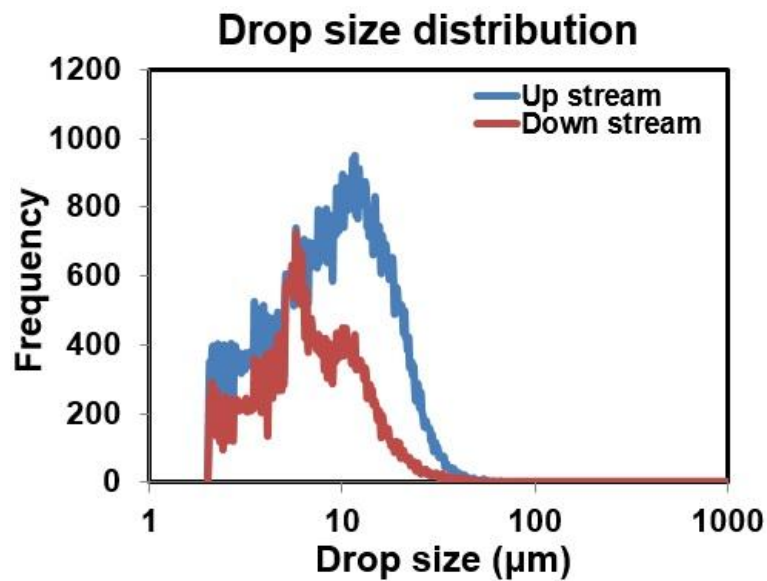


Figure 10. Water droplet diameter distribution from upstream and downstream samples of beaded fibers.

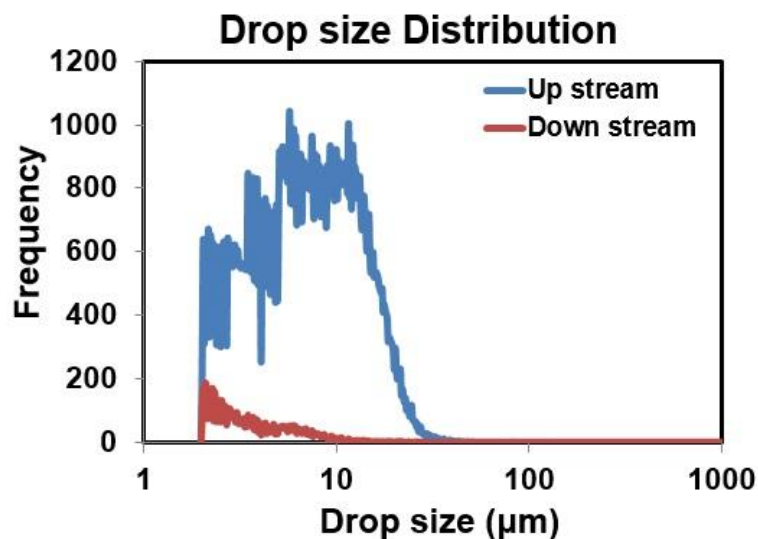


Figure 11. Droplet diameter distribution from upstream and downstream samples of non-beaded fibers.

#### 4. Conclusions

The electrospinning process is a useful process to fabricate nanoscale filaments from polymeric solution. The morphologies of the electrospun fibers are dependent upon the electrospinning conditions and the composition of the electrospinning solution. In this work, the addition of different salts and surfactants to the polyetherimide (PEI) electrospinning solution for fabricating polyetherimide (PEI) with better morphology was investigated. The results showed that production of PEI electrospun fiber mats without beads was achieved by adding 1 wt. % or higher of HTAB surfactant to the electrospinning solution. PEI fiber mats without beads, compared to mats with beads, had better thermal properties, mechanical properties, permeability, and separation performance in liquid-liquid filtration tests. Thus, the addition of 1 wt. % HTAB to the PEI electrospinning solution greatly improved the fiber mat properties.

**Acknowledgments:** The authors would like to sincerely thank Jazan University, Saudi Arabia, and SABIC for supporting this project. We also would like to thank Royal Commission for Jubail and Yanbu for sponsoring A. Aljuhani and Coalescence Filtration Nanofibers Consortium (Ahlstrom, Bekaert, Cummins Filtration,

Donaldson, Hollingsworth & Vose, Parker-Hannifin Corporation and SNS Nanofiber Technology) for financial support of this research.

**Author Contributions:** Ahmed Abutaleb, Dinesh Lolla collectively designed, conducted experiments and wrote the paper. Abdulwahab Aljuhani designed filter holder and apparatus for diesel-water experiments. Hyeon U. Shin and Jonathan W. Rajala conducted SEM and mechanical analysis. George G. Chase advised the work.

**Conflicts of Interest:** The authors declare no conflict of interest.

## References

1. Ko, F.K.; Yang, H. Functional Nanofibre: Enabling Material for the Next Generations Smart Textiles. *J. Fiber Bioeng. Inf.* **2008**, *1*, 81–92. [[CrossRef](#)]
2. Lolla, D.; Gorse, J.; Kisielowski, C.; Miao, J.; Taylor, P.L.; Chase, G.G.; Reneker, D.H. Polyvinylidene fluoride molecules in nanofibers, imaged at atomic scale by aberration corrected electron microscopy. *Nanoscale* **2015**, *8*, 120–128. [[CrossRef](#)] [[PubMed](#)]
3. Shin, H.U.; Abutaleb, A.; Lolla, D.; Chase, G.G. Effect of Calcination Temperature on NO–CO Decomposition by Pd Catalyst Nanoparticles Supported on Alumina Nanofibers. *Fibers* **2017**, *5*, 22. [[CrossRef](#)]
4. Subbiah, T.; Bhat, G.S.; Tock, R.W.; Parameswaran, S.; Ramkumar, S.S. Electrospinning of nanofibers. *J. Appl. Polym. Sci.* **2005**, *96*, 557–569. [[CrossRef](#)]
5. Shahreen, L.; Chase, G.G.; Turinske, A.J.; Nelson, S.A.; Stojilovic, N. NO decomposition by CO over Pd catalyst supported on TiO<sub>2</sub> nanofibers. *Chem. Eng. J.* **2013**, *225*, 340–349. [[CrossRef](#)]
6. Frenot, A.; Chronakis, I.S. Polymer nanofibers assembled by electrospinning. *Curr. Opin. Colloid Interface Sci.* **2003**, *8*, 64–75. [[CrossRef](#)]
7. Nayak, R.; Padhye, R.; Kyratzis, I.L.; Truong, Y.B.; Arnold, L. Recent advances in nanofibre fabrication techniques. *Text. Res. J.* **2012**, *82*, 129–147. [[CrossRef](#)]
8. Gibson, P.W.; Schreuder-Gibson, H.L.; Rivin, D. Electrospun fiber mats: Transport properties. *AIChE J.* **1999**, *45*, 190–195. [[CrossRef](#)]
9. Huang, Z.M.; Zhang, Y.Z.; Kotaki, M.; Ramakrishna, S. A review on polymer nanofibers by electrospinning and their applications in nanocomposites. *Compos. Sci. Technol.* **2003**, *63*, 2223–2253. [[CrossRef](#)]
10. Ramaseshan, R.; Sundarrajan, S.; Jose, R.; Ramakrishna, S. Nanostructured ceramics by electrospinning. *J. Appl. Phys.* **2007**, *102*, 1–17. [[CrossRef](#)]
11. Hartgerink, J.D.; Beniash, E.; Stupp, S.I. Self-assembly and mineralization of peptide-amphiphile nanofibers. *Science* **2001**, *294*, 1684–1688. [[CrossRef](#)] [[PubMed](#)]
12. Liang, H.; Guan, Q.; Chen, L.; Zhu, Z.; Zhang, W.; Yu, S. Macroscopic-Scale Template Synthesis of Robust Carbonaceous Nanofiber Hydrogels and Aerogels and Their Applications. *Angew. Chem.* **2012**, *51*, 5101–5105. [[CrossRef](#)] [[PubMed](#)]
13. Zhao, J.; Han, W.; Chen, H.; Tu, M.; Zeng, R.; Shi, Y.; Cha, Z.; Zhou, C. Preparation, structure and crystallinity of chitosan nanofibers by a solid-liquid phase separation technique. *Carbohydr. Polym.* **2011**, *83*, 1541–1546. [[CrossRef](#)]
14. Grande, R.; Trovatti, E.; Gandini, A.; Carvalho, A.J.F. Continuous microfiber drawing by interfacial charge complexation between anionic cellulose nano fibers and cationic chitosan. *J. Mater. Chem. A* **2017**, *5*, 13098–13103. [[CrossRef](#)]
15. Suzuki, A.; Hosoi, K.; Miyagi, K. Broad poly(ethylene terephthalate) nanofiber sheet prepared by CO<sub>2</sub> laser supersonic continuous multi-drawing. *Polymer* **2015**, *60*, 252–259. [[CrossRef](#)]
16. Aruna, S.T.; Balaji, L.S.; Kumar, S.S.; Prakash, B.S. Electrospinning in solid oxide fuel cells—A review. *Renew. Sustain. Energy Rev.* **2017**, *67*, 673–682. [[CrossRef](#)]
17. Mercante, L.A.; Scagion, V.P.; Migliorini, F.L.; Mattoso, L.H.C.; Correa, D.S. Trends in Analytical Chemistry Electrospinning-based (bio) sensors for food and agricultural applications: A review. *Trends Anal. Chem.* **2017**, *91*, 91–103. [[CrossRef](#)]
18. Shin, H.U.; Lolla, D.; Nikolov, Z.; Chase, G.G. Pd–Au nanoparticles supported by TiO<sub>2</sub> fibers for catalytic NO decomposition by CO. *J. Ind. Eng. Chem.* **2016**, *33*, 91–98. [[CrossRef](#)]
19. Rajala, J.; Shin, H.U.; Lolla, D.; Chase, G. Core–Shell Electrospun Hollow Aluminum Oxide Ceramic Fibers. *Fibers* **2015**, *3*, 450–462. [[CrossRef](#)]



20. Lolla, D.; Lolla, M.; Abutaleb, A.; Shin, H.U.; Reneker, D.H.; Chase, G.G. Fabrication, polarization of electrospun polyvinylidene fluoride electret fibers and effect on capturing nanoscale solid aerosols. *Materials* **2016**, *9*, 671. [[CrossRef](#)] [[PubMed](#)]
21. Kriegel, C.; Kit, K.M.; McClements, D.J.; Weiss, J. Influence of surfactant type and concentration on electrospinning of chitosan-poly(ethylene oxide) blend nanofibers. *Food Biophys.* **2009**, *4*, 213–228. [[CrossRef](#)]
22. Lin, T.; Wang, H.; Wang, H.; Wang, X. The charge effect of cationic surfactants on the elimination of fibre beads in the electrospinning of polystyrene. *Nanotechnology* **2004**, *15*, 1375–1381. [[CrossRef](#)]
23. Araujo, E.S.; Nascimento, M.L.F.; de Oliveira, H.P. Influence of triton X-100 on PVA fibres production by the electrospinning technique. *Fibres Text. East. Eur.* **2013**, *100*, 39–43.
24. Fong, H.; Chun, I.; Reneker, D.H. Beaded nanofibers formed during electrospinning. *Polymer* **1999**, *40*, 4585–4592. [[CrossRef](#)]
25. Arayanarakul, K.; Choktaweasap, N.; Aht-ong, D.; Meechaisue, C.; Supaphol, P. Effects of poly(ethylene glycol), inorganic salt, sodium dodecyl sulfate, and solvent system on electrospinning of poly(ethylene oxide). *Macromol. Mater. Eng.* **2006**, *291*, 581–591. [[CrossRef](#)]
26. Fallahi, D.; Rafizadeh, M.; Mohammadi, N.; Vahidi, B. Effect of LiCl and non-ionic surfactant on morphology of polystyrene electrospun nanofibers. *E-Polymers* **2008**, *8*, 1–10. [[CrossRef](#)]
27. Ye, H.; Huang, J.; Xu, J.; Khalfan, A.; Greenbaum, S.G. Li Ion Conducting Polymer Gel Electrolytes Based on Ionic Liquid/PVDF-HFP Blends. *J. Electrochem. Soc.* **2007**, *154*, 1048–1057. [[CrossRef](#)]
28. Nartetamrongsutt, K.; Chase, G.G. The influence of salt and solvent concentrations on electrospun polyvinylpyrrolidone fiber diameters and bead formation. *Polymer* **2013**, *54*, 2166–2173. [[CrossRef](#)]
29. Goh, Y.-F.; Shakir, I.; Hussain, R. Electrospun fibers for tissue engineering, drug delivery, and wound dressing. *J. Mater. Sci.* **2013**, *48*, 3027–3054. [[CrossRef](#)]
30. Yao, L.; Hass, T.W.; Bowlin, L. Electrospinning and Stabilization of Fully Hydrolyzed Poly(Vinyl Alcohol) Fibers. *Chem. Mater.* **2003**, *15*, 1860–1864. [[CrossRef](#)]
31. Scarlet, R.; Manea, L.R.; Sandu, I.O.N.; Martinova, L.; Cramariuc, O. Study on the Solubility of Polyetherimide for Nanostructural Electrospinning. *Rev. Chim.* **2012**, *63*, 688–692.
32. Singh, D.; Rezac, M.E.; Pfromm, P.H. Partial hydrogenation of soybean oil with minimal trans fat production using a pt-decorated polymeric membrane reactor. *JAOCs J. Am. Oil Chem. Soc.* **2009**, *86*, 93–101. [[CrossRef](#)]
33. Yousef, A.; Brooks, R.M.; El-Halwany, M.M.; Abutaleb, A.; El-Newehy, M.H.; Al-Deyab, S.S.; Kim, H.Y. Electrospun CoCr<sub>7</sub>C<sub>3</sub>-supported C nanofibers: Effective, durable, and chemically stable catalyst for H<sub>2</sub> gas generation from ammonia borane. *Mol. Catal.* **2017**, *434*, 32–38. [[CrossRef](#)]
34. Yousef, A.; Brooks, R.M.; Abutaleb, A.; El-newehy, M.H. One-step synthesis of Co-TiC-carbon composite nanofibers at low temperature. *Ceram. Int.* **2017**, *43*, 5828–5831. [[CrossRef](#)]
35. Patel, S.U.; Chase, G.G. Separation of water droplets from water-in-diesel dispersion using superhydrophobic polypropylene fibrous membranes. *Sep. Purif. Technol.* **2014**, *126*, 62–68. [[CrossRef](#)]
36. Patel, S.U.; Patel, S.U.; Chase, G.G. Electrospun superhydrophobic poly(vinylidene fluoride-co-hexafluoropropylene) fibrous membranes for the separation of dispersed water from ultralow sulfur diesel. *Energy Fuels* **2013**, *27*, 2458–2464. [[CrossRef](#)]
37. Viswanadam, G.; Chase, G.G. Water–diesel secondary dispersion separation using superhydrophobic tubes of nanofibers. *Sep. Purif. Tech.* **2013**, *104*, 81–88. [[CrossRef](#)]
38. Yang, X.; Zhang, X.; Wang, H.; Chase, G.G. Vibration assisted water-diesel separation by electrospun PVDF-HFP fiber mats. *Sep. Purif. Tech.* **2016**, *171*, 280–288. [[CrossRef](#)]
39. Moon, S.C.; Choi, J.K.; Farris, R.J. Preparation of Aligned Polyetherimide Fiber by Electrospinning. *J. Appl. Polym. Sci.* **2008**, *109*, 691–694. [[CrossRef](#)]
40. Choi, S.S.; Lee, S.G.; Joo, C.W.; Im, S.S.; Kim, S.H. Formation of interfiber bonding in electrospun poly(etherimide) nanofiber web. *J. Mater. Sci.* **2004**, *39*, 1511–1513. [[CrossRef](#)]

